Int. J. Solids Structures, 1975, Vol. 11, pp. 1097–1110. Pergamon Press. Printed in Great Britain

HIGH-ORDER TRIANGULAR FINITE ELEMENT FOR SHELL ANALYSIS

D. J. DAWE
Department of Civil Engineering, University of Birmingham, Birmingham, England

(*Received* 8 *August* 1974; *revised* 18 *February* 1975)

Abstract—A curved-shell finite element of triangular shape is described which is based on conventional shell theory expressed in terms of surface coordinates and displacements. Each of the three surface displacement components is independently represented by a two-dimensional polynomial of constrained-quintic order giving the element a total of 54 degrees of freedom. Two particular geometric forms of the element are considered, viz. doubly-curved shallow and circular cylindrical. The high level of accuracy which can be achieved using few elements is demonstrated in a range of problems where comparison is made with previous finite element solutions.

1. INTRODUCTION

Recent studies by the author[1, 2] of the comparative efficiency of various arch finite elements have demonstrated the characteristics of models based both on relatively high-order polynomial displacement fields and on assumed-strain fields. Arch models based on (two) independently-interpolated displacement components of quintic order have been shown to be consistently very efficient in a range of applications embracing shallow and deep geometries and extensional and nearly-inextensional behaviour. This efficiency is such that in modelling circular arches with a single element based on surface (i.e. tangential and normal) quintic displacement components the error in the calculated maximum displacement is less than 0·4% in any of the considered applications[2]; calculated forces and bending moments are also accurate. Elements based on polynomial displacement fields in which one or both components is reduced to cubic order are very much less efficient on a degree-of-freedom as well as on an element basis. In particular, if the tangential component is restricted to a cubic variation element efficiency depends markedly on problem geometry and the calculated force distributions for such models exhibit waviness in all applications; this waviness becomes very pronounced in nearly-inextensional problems where its order can be very many times greater than the true magnitude of the force. This is so whether the associated normal component of displacement is of cubic or quintic order and, in general, there is no improvement in increasing the order of the normal component from cubic to quintic unless the order of the tangential component is similarly increased (though exceptionally there is a significant improvement where the arch geometry is shallow and relatively thick).

The arch studies point to the use of quintic polynomial displacement components as the basis for doubly-curved shell elements. In fact there already exist in the literature two conforming elements of triangular planform with quintic polynomial assumptions for all three displacement components[3, 4] but these components are cartesian ones. Cartesian displacement components were chosen since they allow the precise representation of the rigid-body motions of an element when the geometry of the undeformed shell is defined by linear combinations of the same set of basic functions used to define the displacements. In the work of Argyris and Scharpf[3] the development of the shell theory on which the element is based uses the natural strain concept and its relationship to classical thin shell theory is not obvious. The work of Dupuis and Goël[4] is based on shell theory written in terms of a cartesian coordinate system in place of the usual curvilinear system and the equations are expressed in relation to the height of the curved middle surface above a reference plane. Possible difficulties associated with such schemes as these have been pointed out by Morris[5]. In a further study Dupuis[6] has described a triangular shell element based on a modified representation of the shell geometry in which the element is straight-sided in the plane of shell parameters. Rigid-body motions are represented precisely only by making an appropriate approximation to the shell middle surface and although the derivation is, in principle, quite general it is specialised to the case where the displacement components are represented by third-order polynomials.

As shown by the results for circular arches[2] the exact representation of element rigid-body motion states (whose nature is discussed in [7]) or indeed of other basic states such as inextensional modes, is not necessary for high accuracy and rapid convergence providing such states can be closely approximated. This can be achieved in an element based on conventional shell theory and the assumption of independently-interpolated polynomial surface components so long as the order of the polynomial components is sufficiently high. It is further noted that polynomial surface displacement fields are particularly appropriate in dealing with an important class of "sensitive" problems in shell work[5, 8] and that an analysis based on conventional theory easily allows the exact geometric representation of standard shapes of shell.

The present paper details the development and application of a conforming triangular shell element which belongs to the category described in the preceding paragraph. The order of each surface component polynomial is constrained-quintic (i.e. basically a complete quintic polynomial in two dimensions having twenty-one terms to which three constraints are applied) and thus the element has a total of 54 degrees of freedom. The philosophy is a general one but here the analysis is limited to two specific classes of shell geometry which exhibit the characteristics of general shells, viz. the shallow shell with two principal radii of curvature plus a radius of twist and the circular cylindrical shell. This restriction is imposed so that the element stiffness may be obtained in closed form and numerical integration avoided. The elimination of any possible small error associated with a numerical integration scheme is considered desirable since it is proposed to study in detail the precise variation of calculated displacements, membrane forces and bending moments over the shell middle surface.

The approach described here is directly related to that adopted earlier by Cowper, Lindberg and Olson[9–12] with the fundamental difference that whilst the earlier work is based on the assumption of a constrained-quintic normal displacement component, the two tangential displacement components are taken to be cubic polynomials. Cowper *et al.*[12] contend that, for a set number of elements, increasing the order of the tangential components to constrained quintic will lead to only a marginal improvement in accuracy achieved at the expense of an increase in the degrees of freedom of 50%. This contention is based on error considerations using a Taylor's series but is certainly not correct in all situations since, as mentioned earlier, in the limiting case of the deep circular arch a model with quintic tangential displacement is much more efficient on a degree-of-freedom basis than a corresponding model with cubic tangential displacement.

Any assessment of the merits of a finite element proposed for the analysis of shell structures must take account of the diversity of possible applications of the element. Depending upon geometry and loading the shell response may be dominated by membrane behaviour, or by bending behaviour, or the shell might function primarily as a membrane with local zones of bending, etc.; rigid-body motions may or may not be of importance. In these circumstances a valid theoretical prediction of the accuracy of a finite element modelling of a general curved shell structure with large, unequal elements, is very difficult to construct. (It is noted though that detailed error estimates have been presented for the simplified problem of the circular arch[13–15]). Accordingly, the accuracy of the element presented here is examined solely by numerical application to specific problems. However, such applications, supplemented by results presented earlier for the limiting case of the arch[1, 2], embrace a wide range of shell behaviour which includes all the categories noted above. In the presentation of detailed numerical results particular attention is paid to a comparison between results of the present analysis and that of Cowper *et al.* in a range of applications. It would be expected from the arch results that there would be a significant improvement in solution efficiency using the 54 degree-of-freedom (54 dof) element in many deep, thin situations but a lesser improvement in shallow applications.

Finally, it is noted that at the review stage one of the referees of this paper has drawn attention to some recent work of Idelsohn[16] in which a family of shell elements related to that described herein is apparently developed.

2. ANALYSIS DETAILS

Of the many shell theories available in the literature that of Koiter[17] is adopted here. In this theory (unlike some others) the homogeneous strain-displacement equations are satisfied in a general rigid-body motion. The theory assumes an orthogonal curvilinear coordinate system but this system need not coincide with the lines of principal curvature of the shell surface, or the

notation of Koiter the strain energy density, dV_0, of a shell of thickness h may be expressed as the sum of the extensional and flexural energies in the form

$$dV_0 = \frac{1}{2} C \left(\left[(\epsilon_1 + \epsilon_2)^2 - 2(1-\nu) \left(\epsilon_1 \epsilon_2 - \frac{1}{4} \psi^2 \right) \right] + \frac{h^2}{12} [(\chi_1 + \chi_2)^2 - 2(1-\nu)(\chi_1 \chi_2 - \tau^2)] \right)$$

or

$$dV_0 = \frac{C}{2} [\epsilon][B]\{\epsilon\}. \tag{1}$$

Here

$$\{\epsilon\} = \{\epsilon_1, \epsilon_2, \psi, \chi_1, \chi_2, \tau\} \tag{2}$$

and the (6×6) matrix $[B]$ is easily constructed. The quantities ϵ_1 and ϵ_2 are the extensional strains along orthogonal parametric curves α, β and ψ is the shear strain between these curves; χ_1, χ_2 and τ are the physical components of the changes of curvature and twist referred to these curves. Also the quantity C is defined as

$$C = \frac{Eh}{(1-\nu^2)}$$

where E and ν are Young's modulus and Poisson's ratio respectively.

As mentioned earlier, the present paper is concerned specifically with two representative types of shell—those of shallow geometry and those of circular cylindrical geometry—so that simplified strain-displacement equations can be used and thus the element stiffness can be evaluated in closed form. For both types of shell the strain-displacement equations can be conveniently expressed as

$$\{\epsilon\} = [D]\{d\} \tag{3}$$

where

$$\{d\} = \left\{ \frac{\partial U}{\partial X}, \frac{\partial U}{\partial Y}, \frac{\partial V}{\partial X}, \frac{\partial V}{\partial Y}, W, \frac{\partial^2 W}{\partial X^2}, \frac{\partial^2 W}{\partial X \partial Y}, \frac{\partial^2 W}{\partial Y^2} \right\}. \tag{4}$$

For the shallow shell U and V are the tangential displacement components in directions parallel to suitable global cartesian coordinates X and Y, and W is the normal displacement component. Following the usual assumptions of shallow shell theory, the matrix $[D]$ is

$$[D] = \begin{bmatrix} 1 & 0 & 0 & 0 & 1/R_1 & 0 & 0 & 0 \\ 0 & 0 & 0 & 1 & 1/R_2 & 0 & 0 & 0 \\ 0 & 1 & 1 & 0 & 2/T & 0 & 0 & 0 \\ 0 & 0 & 0 & 0 & 0 & 1 & 0 & 0 \\ 0 & 0 & 0 & 0 & 0 & 0 & 0 & 1 \\ 0 & 0 & 0 & 0 & 0 & 0 & 1 & 0 \end{bmatrix} \tag{5}$$

where R_1, R_2 and T are the (constant) radii of curvature and twist of the middle surface related to the X, Y coordinates.

For the cylindrical shell the X coordinate runs parallel to the longitudinal axis and Y is the curvilinear coordinate orthogonal to X; U, V and W are displacement components in the directions of the X coordinate, Y coordinate and the shell normal respectively. The matrix $[D]$ in this case is taken to be

$$[D] = \begin{bmatrix} 1 & 0 & 0 & 0 & 0 & 0 & 0 & 0 \\ 0 & 0 & 0 & 1 & 1/R & 0 & 0 & 0 \\ 0 & 1 & 1 & 0 & 0 & 0 & 0 & 0 \\ 0 & 0 & 0 & 0 & 0 & 1 & 0 & 0 \\ 0 & 0 & 0 & -1/R & 0 & 0 & 0 & 1 \\ 0 & \frac{1}{4}R & -\frac{3}{4}R & 0 & 0 & 0 & 1 & 0 \end{bmatrix} \tag{6}$$

where R is the mean radius of the cylinder.

For the finite element analysis the domain of the shell in the XY plane (representing the base plane in the case of the shallow shell or the developed plane for the cylindrical shell) is divided into triangular elements as shown in Fig. 1. Within an element it is required that each of the three displacement components varies basically as a quintic polynomial in the two coordinates. As is well known, the use of a quintic polynomial displacement field originated in the development of refined conforming triangular plate bending elements by a number of independent investigators (see [18]). Corresponding to a complete quintic polynomial such an element has twenty-one degrees of freedom comprising the deflection with its first and second derivatives at each vertex together with the normal derivative at the mid-point of each side. However, a more convenient eighteen dof (constrained-quintic) displacement field is obtained when the mid-side degrees of freedom are eliminated by restricting the variation of normal slope along an edge to a cubic polynomial and it is the constrained-quintic polynomial which is selected here for each displacement component. Connection of all nodal quantities ensures continuity at inter-element boundaries of each displacement component and of its normal derivative, although the continuity of the normal derivative of the tangential components is not strictly necessary for compliance with the potential energy principle.

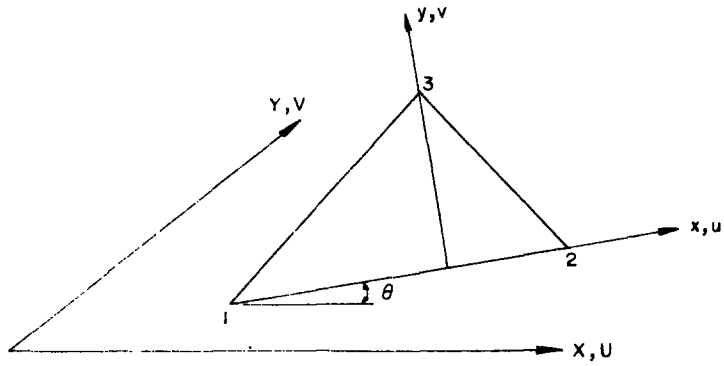

Fig. 1. Shell element in X–Y plane.

Having decided in broad terms the basis of the shell element the detailed calculation of the element stiffness can be implemented in a number of ways, but it is most convenient here to extend and modify the approach described by Cowper *et al.* [9, 10]. This approach leads to a general closed-form integration formula for the evaluation of stiffness terms via the introduction of local coordinate axes x and y (see Fig. 1). The corresponding local displacement components are the tangential ones u and v measured in the directions of x and y respectively, together with the component normal to the shell surface, w, which coincides with the global component, W.

The components of the conforming displacement field are assumed to be of the form

$$\begin{aligned} u = {} & A_1 + A_2x + A_3y + A_4x^2 + A_5xy + A_6y^2 + A_7x^3 + A_8x^2y \\ & + A_9xy^2 + A_{10}y^3 + A_{11}x^4 + A_{12}x^3y + A_{13}x^2y^2 + A_{14}xy^3 \\ & + A_{15}y^4 + A_{16}x^5 + A_{17}x^4y + A_{18}x^3y^2 + A_{19}x^2y^3 + A_{20}xy^4 + A_{21}y^5 \end{aligned}$$

with like expressions for v and w giving 60 independent coefficients A_i in all. The displacement components are more suitably expressed

$$u = \sum_{i=1}^{20} A_i x^{m_i} y^{n_i}, \quad v = \sum_{i=21}^{40} A_i x^{p_i} y^{q_i} \quad \text{and} \quad w = \sum_{i=41}^{60} A_i x^{r_i} y^{s_i} \tag{7}$$

where $m_i \ldots s_i$ are integers running between 0 and 5. The above polynomial does not contain an x^4y term so that the normal slope variation along edge 1–2 is automatically restricted to a cubic polynomial; two further constraint conditions per component are applied later to similarly restrict the normal slope variation along the remaining edges. The number of independent coefficients is thus reduced to 18 per component, 54 in all.

Following the example of [10] the strain energy for the shallow or the cylindrical shell element can then be expressed (by substituting eqn (5) or (6) into eqn (1) via eqn (3) and transforming to local displacements and coordinates) in the form of an integral over local coordinates as

$$V_0 = \frac{C}{2}\int\int [\tilde{d}][\tilde{L}]\{\tilde{d}\}\,dx\,dy \tag{8}$$

where

$$\{\tilde{d}\} = \left\{\frac{\partial u}{\partial x}, \frac{\partial u}{\partial y}, \frac{\partial v}{\partial x}, \frac{\partial v}{\partial y}, w, \frac{\partial^2 w}{\partial x^2}, \frac{\partial^2 w}{\partial x \partial y}, \frac{\partial^2 w}{\partial y^2}\right\} \tag{9}$$

and

$$[\tilde{L}] = [R_4]^T[D]^T[B][D][R_4]. \tag{10}$$

Matrices $[R_4]$ and $[\tilde{L}]$ have the same general meaning here as in [10]; the rotation matrix $[R_4]$, which links the column vectors $\{d\}$ and $\{\tilde{d}\}$ (i.e. $\{d\} = [R_4]\{\tilde{d}\}$) is in fact unchanged whilst matrix $[\tilde{L}]$ does, of course, differ in detail both between the shallow and cylindrical shell analyses described here and the earlier analysis.

The strain energy can be further expressed via eqn (7) in the form

$$V_0 = \frac{C}{2}[A][k]\{A\}. \tag{11}$$

Here $\{A\}$ is the column vector of the sixty coefficient A_i and $[k]$ is a (60×60) "stiffness" matrix whose elements k_{ij} are explicitly defined in terms of the elements of the (8×8) matrix $[\tilde{L}]$ by a modified form of the equation given in the Appendix of [10]. Since this modified equation is a long one it will not be presented in full here; rather the necessary changes from the original equation will be noted.

For the shallow shell element described here the expression for k_{ij} is that of the original equation but rows 8 to 13 inclusive as printed may be deleted since the elements of matrix $[L]$ which are involved (L (1,6) through to L (4,8)) are in this case zero. For the cylindrical shell element presented here the expression for k_{ij} is the complete one of [10] with the addition of the two terms

$$\begin{aligned} &+\tilde{L}(6,7)[r_i(r_i-1)r_j s_j + r_j(r_j-1)r_i s_i]F(r_i+r_j-3, s_i+s_j-1) \\ &+\tilde{L}(7,8)[r_i s_i s_j(s_j-1) + r_j s_j s_i(s_i-1)]F(r_i+r_j-1, s_i+s_j-3) \end{aligned} \tag{12}$$

where $F(m, n)$ is defined in [10].

The "stiffness" matrix $[k]$ corresponds to the quadratic form (eqn 11) of the strain energy in terms of the polynomial coefficients $\{A\}$. The energy can be further expressed in a quadratic form of the global degrees of freedom as

$$V_0 = \frac{C}{2}[W_2][K_2]\{W_2\} \tag{13}$$

where,

$$[K_2] = [R]^T[T_1]^T[k][T_1][R] \tag{14}$$

is the required global stiffness matrix.

Here the column vector of global degrees of freedom $\{W_2\}$ of length 54 comprises the quantities

$$U, \frac{\partial U}{\partial X}, \frac{\partial U}{\partial Y}, \frac{\partial^2 U}{\partial X^2}, \frac{\partial^2 U}{\partial X \partial Y}, \frac{\partial^2 U}{\partial Y^2}, \quad V \cdots\cdots \frac{\partial^2 V}{\partial Y^2}, W \cdots\cdots \frac{\partial^2 W}{\partial Y^2}$$

at each of nodes 1, 2 and 3 in turn. The matrices $[T_1]$ and $[R]$ here, of course, take a different form from that used in the work of Cowper *et al.*[9, 10]. Matrix $[T_1]$ is a transformation matrix relating the coefficients A_i to the local degrees of freedom, $u, (\partial u/\partial x), \ldots, (\partial^2 w/\partial y^2)$ at each node, using the boundary conditions and incorporating the two constraint equations per displacement component which are required, as mentioned above, to restrict the normal slope variation along edges 2–3 and 3–1. Matrix $[T_1]$ is of order (60×54) and is the inverse of a (60×60) matrix $[T]$ with the last six columns of this inverse deleted: details of matrix $[T]$ are given in Table 1. Matrix $[R]$ is a rotation matrix used to transform global degrees of freedom to local ones and is detailed in Table 2.

Table 1. Matrix $[T]$, where submatrices $[S_2]$, $[S_4]$, $[S_6]$ and $[S_8]$ are as defined in [9]

$$[T] = \begin{bmatrix} S_2 & 0 & 0 \\ 0 & S_2 & 0 \\ 0 & 0 & S_2 \\ S_4 & 0 & 0 \\ 0 & S_4 & 0 \\ 0 & 0 & S_4 \\ S_6 & 0 & 0 \\ 0 & S_6 & 0 \\ 0 & 0 & S_6 \\ S_8 & 0 & 0 \\ 0 & S_8 & 0 \\ 0 & 0 & S_8 \end{bmatrix}$$

Table 2. Matrix $[R]$

$$[R] = \begin{bmatrix} r_1 & 0 & 0 & 0 & 0 & 0 \\ 0 & r_2 & 0 & 0 & 0 & 0 \\ 0 & 0 & r_1 & 0 & 0 & 0 \\ 0 & 0 & 0 & r_2 & 0 & 0 \\ 0 & 0 & 0 & 0 & r_1 & 0 \\ 0 & 0 & 0 & 0 & 0 & r_2 \end{bmatrix}$$

where

$$[r_1] = \begin{bmatrix} c & 0 & 0 & 0 & 0 & 0 & s & 0 & 0 & 0 & 0 & 0 \\ 0 & c^2 & sc & 0 & 0 & 0 & 0 & sc & s^2 & 0 & 0 & 0 \\ 0 & -sc & c^2 & 0 & 0 & 0 & 0 & -s^2 & sc & 0 & 0 & 0 \\ 0 & 0 & 0 & c^3 & 2sc^2 & s^2c & 0 & 0 & 0 & sc^2 & 2s^2c & s^3 \\ 0 & 0 & 0 & -sc^2 & c^3-s^2c & sc^2 & 0 & 0 & 0 & -s^2c & sc^2-s^3 & s^2c \\ 0 & 0 & 0 & s^2c & -2sc^2 & c^3 & 0 & 0 & 0 & s^3 & -2s^2c & sc^2 \\ -s & 0 & 0 & 0 & 0 & 0 & c & 0 & 0 & 0 & 0 & 0 \\ 0 & -sc & -s^2 & 0 & 0 & 0 & 0 & c^2 & sc & 0 & 0 & 0 \\ 0 & s^2 & -sc & 0 & 0 & 0 & 0 & -sc & c^2 & 0 & 0 & 0 \\ 0 & 0 & 0 & 0 & 0 & 0 & 0 & 0 & 0 & c^3 & 2sc^2 & s^2c \\ 0 & 0 & 0 & 0 & 0 & 0 & 0 & 0 & 0 & -sc^2 & c^3-s^2c & sc^2 \\ 0 & 0 & 0 & 0 & 0 & 0 & 0 & 0 & 0 & s^2c & -2sc^2 & c^3 \end{bmatrix}$$

$$[r_2] = \begin{bmatrix} 1 & 0 & 0 & 0 & 0 & 0 \\ 0 & c & s & 0 & 0 & 0 \\ 0 & -s & c & 0 & 0 & 0 \\ 0 & 0 & 0 & c^2 & 2sc & s^2 \\ 0 & 0 & 0 & -sc & c^2-s^2 & sc \\ 0 & 0 & 0 & s^2 & -2sc & c^2 \end{bmatrix}$$

and $s = \sin\theta$, $c = \cos\theta$

Finally, the stress resultants (N_1, N_2 and S) and couples (M_1, M_2 and W) are obtained from the calculated strains using the relationships

$$N_1 = C(\epsilon_1 + \nu\epsilon_2), \qquad M_1 = \frac{Ch^2}{12}(\chi_1 + \nu\chi_2),$$
$$N_2 = C(\epsilon_2 + \nu\epsilon_1), \qquad M_2 = \frac{Ch^2}{12}(\chi_2 + \nu\chi_1), \tag{15}$$
$$S = \frac{1}{2}(1-\nu)C\psi, \qquad W = \frac{Ch^2}{12}(1-\nu)\tau.$$

3. NUMERICAL STUDIES

The two forms of the shell element described in the last section have been used in convergence studies of some well-documented problems. The elements are incorporated into the BERSAFE finite element system [19] and calculations have been performed on an IBM 360 series computer using double precision arithmetic throughout. The distributions of displacements, stress resultants and couples are obtained by calculating these quantities at points along the element edges at intervals of one tenth of the side length. In representing a distributed loading the load vector is derived in a consistent manner through virtual work considerations, the necessary integrals being calculated in closed form. In considering the specification of boundary conditions only the necessary kinematic conditions have been applied; no attempt has been made to satisfy any force boundary conditions in addition.

Infinitely-long, clamped circular cylinder

This singly-curved problem, illustrated in Fig. 2, was chosen as a first check on programme validity. With Poisson's ratio $\nu = 0{\cdot}0$ and all longitudinal displacements zero the problem is equivalent to the centrally-loaded, clamped arch. Four geometries are considered corresponding to the two values of the angle β and the two values of thickness shown in the figure. The shallow form of the shell element is used in analysing the problem corresponding to the smallest value of β. Two gridworks are used in this symmetric problem, one being that shown in Fig. 2, and the other a coarse gridwork of similar form but with only 2 elements in the Y direction.

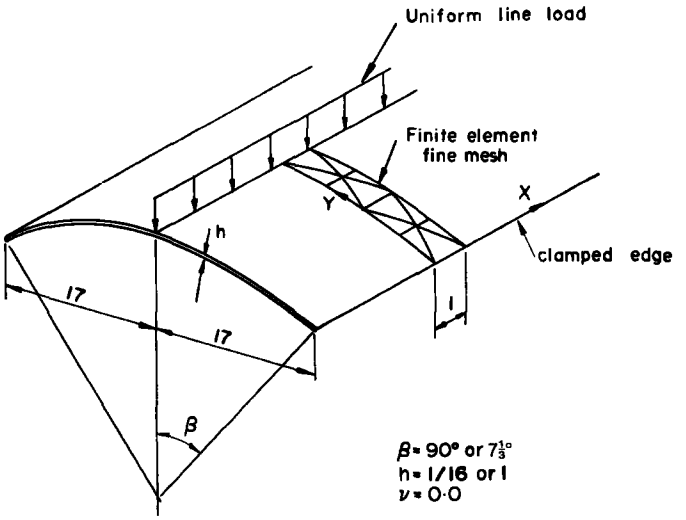

Fig. 2. Details of infinitely-long, clamped cylinder.

The percentage error in the calculated normal deflection under the load for the four geometries is given in Table 3. It is seen that the error increases with increase in angle β and with reduction in thickness. Although the magnitude of the error is small it is generally somewhat larger than that for the corresponding quintic–quintic arch [1, 2] since here in the shell analysis constrained-quintic displacement components are used. It is noted that the numerical studies

Table 3. Error in calculated displacement for infinite cylinder

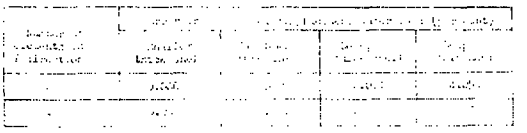

using arch elements show that in this application the efficiency of the shell elements of [9, 10] would be very much less than that of the present elements. For the deep, thin, nearly-inextensional geometry the errors in using two and four quintic-cubic arch elements in the Y direction are in excess of 80% and 10% respectively and these errors will be somewhat increased for the corresponding shell elements since they are based on a constrained-quintic normal displacement component.

Spherical cap

This doubly-curved shallow shell is shown in Fig. 3. The loading is a uniform normal pressure acting over the whole shell surface and the shell edges are freely supported (i.e. W and V zero on edge AD, W and U zero on edge AB). Detailed results for this problem are available for comparison, both exact [20] and based on the 36 dof element of Cowper *et al.* [9]. Two geometries are considered corresponding to values of a shell parameter Rh/L^2 equal to 0·02 and 0·005. Both membrane and bending behaviour are of importance in this difficult problem, the shell functioning primarily as a membrane with zones of bending near the supported edges; these bending zones are more localised for the shell with the smaller value of Rh/L^2 (i.e. for the thinner shell if R and L are constant).

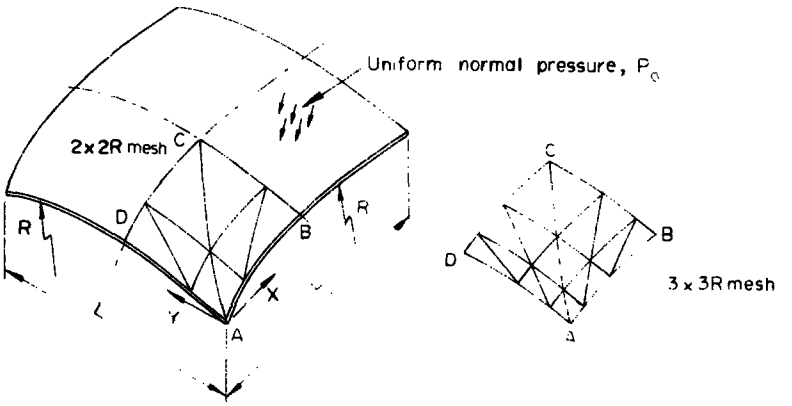

Fig. 3. Spherical cap geometry.

The calculations using the 54 dof shallow element are largely based on the use of a uniform mesh of elements in a symmetric quadrant though this is not the most efficient arrangement in this problem and some use is also made of the refined element meshes shown in Fig. 3. Convergence of the total strain energy calculated for both shell geometries using both the present elements and the 36 dof elements is shown in Fig. 4. It is clear that in this particular shallow application the convergence of the strain energy using the present element is very little different on a degree-of-freedom basis than that of the earlier element.

Some typical distributions of displacements, forces and moments calculated using the 54 dof element are illustrated in Figs. 5a and b where comparison is made with the exact solution. Quite clearly the behaviour of the thinner shell is the more difficult to accommodate in the finite element calculation because of the steeper gradients associated with it. This difficulty is largely overcome by suitable refinement of the mesh and considering the small number of elements that are used in analysing this difficult problem the accuracy of the results is high. The precision of the calculated bending moment distributions presented here is little different from that obtained by Cowper *et al.* [9] but there is a considerable improvement in the calculated force distribution, with much of the oscillation of the force eliminated.

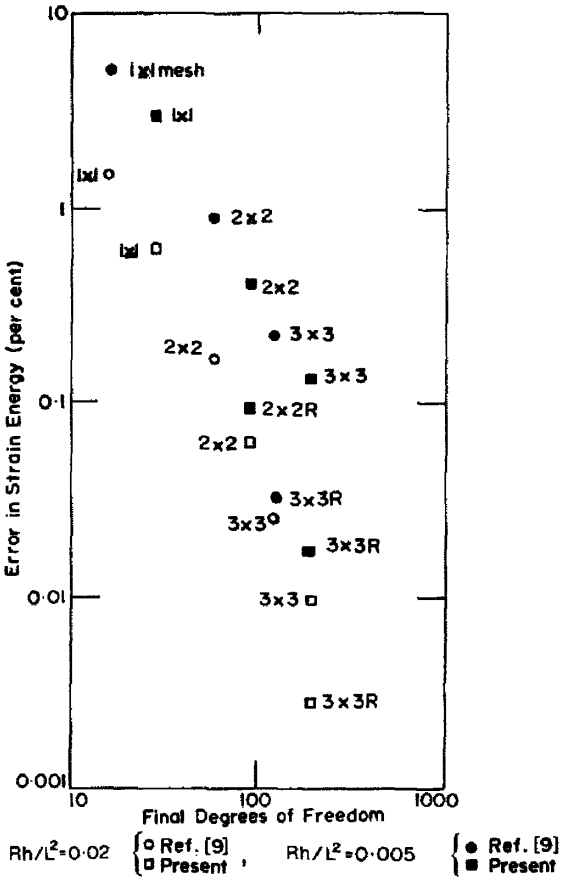

Fig. 4. Convergence of strain energy, spherical cap problem.

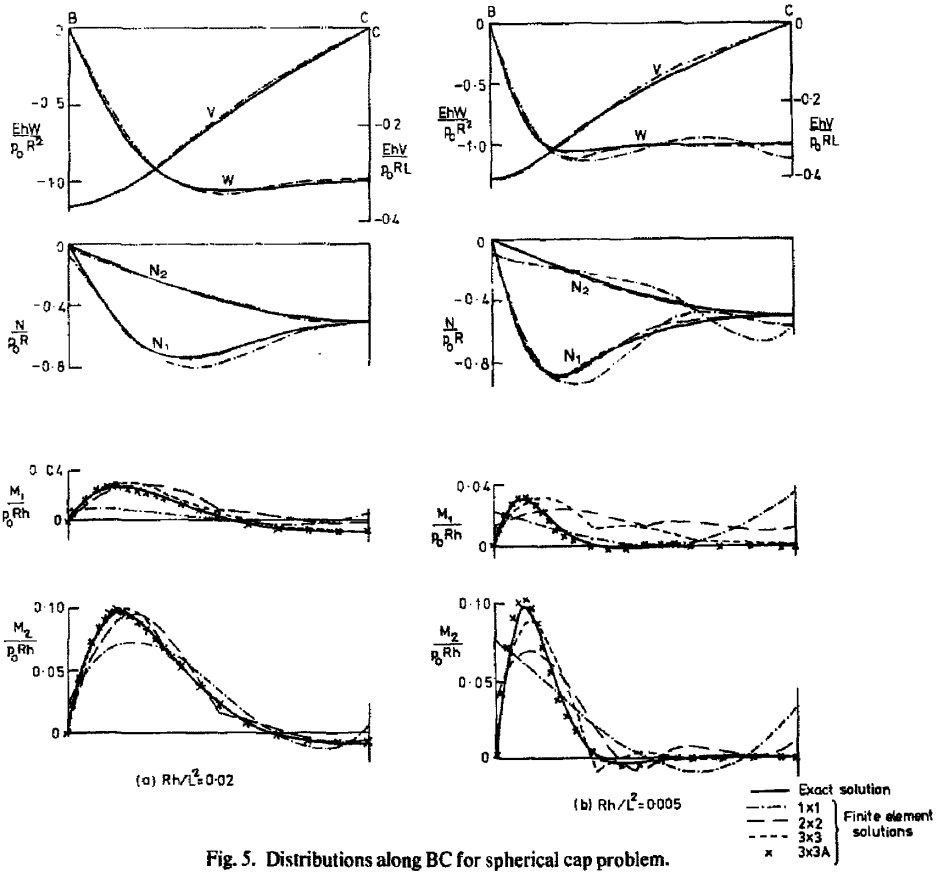

Fig. 5. Distributions along BC for spherical cap problem.

Cylindrical shell roof

The shell roof problem shown in Fig. 6 is a problem which has been used extensively to test finite element analyses. The loading is the self-weight of the shell and membrane and bending effects are both important. The shell is marginally shallow and the "exact" calculations of Scordelis and Lo[21] are largely based on shallow shell equations although not consistently so. A deep shell solution by Forsberg[22] gives a result about 3% lower for the greatest vertical displacement of the shell.

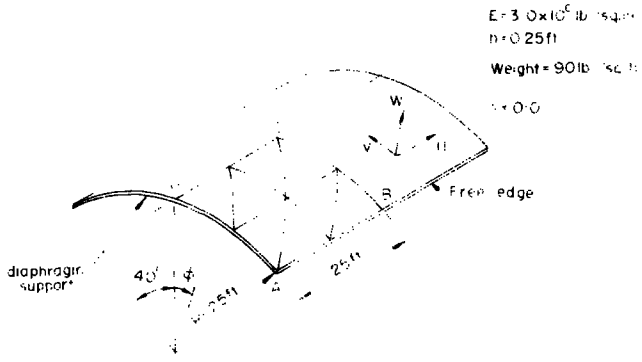

Fig. 6. Shell roof geometry

The shell roof is analysed here using the 54 dof deep cylindrical shell element and uniform element meshes. The self-weight loading is accommodated by resolving into tangential and normal loads of trigonometric form and expressing the sine and cosine of the angle from the vertical as a Taylor's series of terms up to the fourth power of the angle. Distributions of displacement, force and moment at the central section BC are shown in Fig. 7, where it can be seen that the finite element results are very accurate with even the coarsest possible mesh giving generally good agreement with the "exact" results.

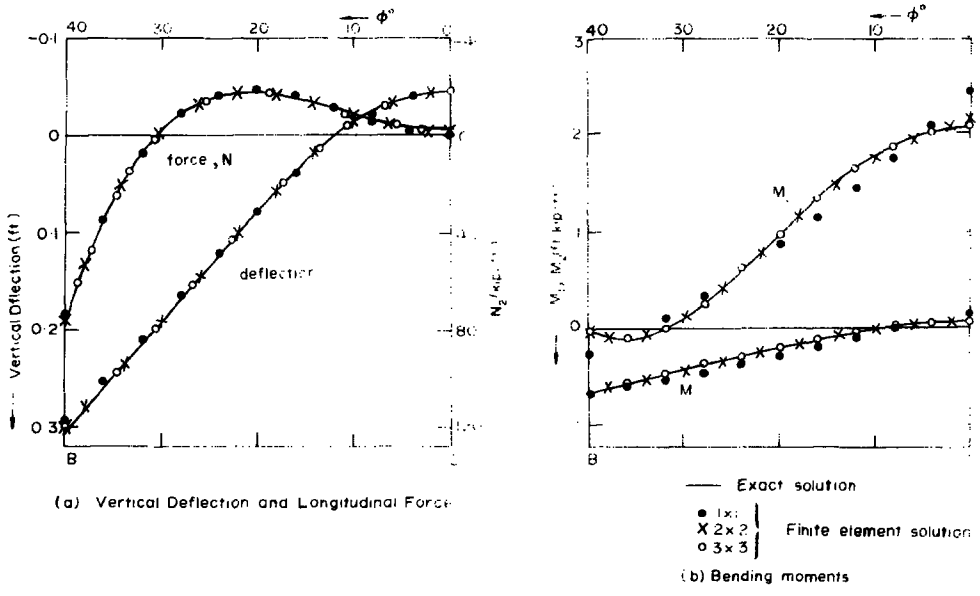

Fig. 7. Shell roof distributions at central section, BC

Details of the rapid convergence of point values of displacement, force and moment and of the total strain energy are recorded in Table 4. Comparative results for an "exact" analysis[9] are listed but since these are based largely on shallow-shell theory convergence is to slightly different levels. It is noted that the rate of convergence of the present finite element results (including particularly that of the strain energy) is much more rapid, on a degree-of-freedom as well as on an

Table 4. Shell roof numerical results

Finite element mesh	$10u_A$ (in.)	w_B (in.)	$10v_B$ (in.)	$10w_C$ (in.)	$10^{-3}(N_1)_B$	$10^{-3}(M_2)_C$ (lb.in./in.)	$10^{-2}(M_1)_C$ (lb.in./in.)	10^{-4} x strain energy (lb.in.)
1 x 1	-1.46502	-3.90142	-8.48344	5.5259	6.0781	2.4520	1.6522	5.69514
2 x 2	-1.48885	-3.97819	-8.61524	5.4483	6.2658	2.1797	1.0615	5.78732
3 x 3	-1.48929	-3.98455	-8.62438	5.4120	6.2982	2.0797	0.9120	5.79115
4 x 4	-1.48345	-3.98432	-8.62556	5.4034	6.3032	2.0627	0.9200	5.79147
Shallow solution [9]	-1.51325	-4.09916	-8.76147	5.2494	6.4124	2.0562	0.9272	5.88277

element basis, than that of the 36 dof element results[9]. This is illustrated for one quantity—the vertical deflection at the centre of the straight edge—in Fig. 8, where results of various other finite element studies[23–25] are also included. The performance of the present element compares well with that of any other available element in this application.

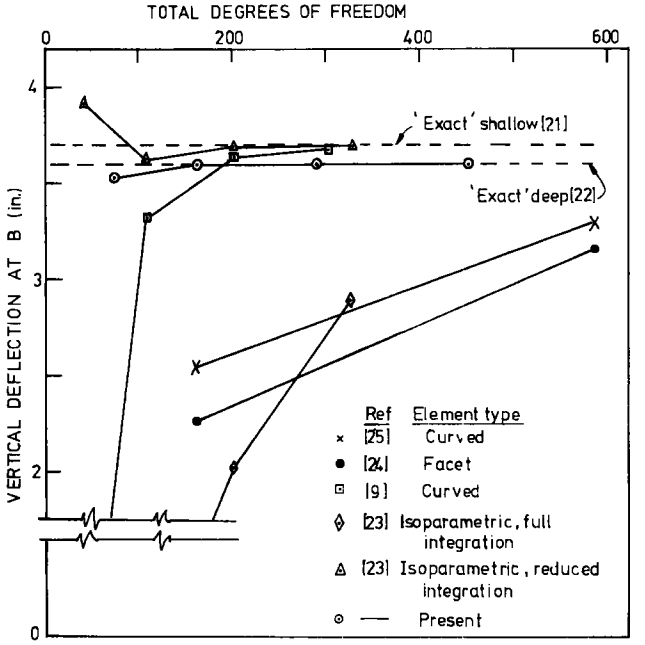

Fig. 8. Shell roof deflection comparison.

Pinched cylinder with free ends

In this problem the ends of the cylinder shown in Fig. 9 are completely free and the relevant data is $L = 10{\cdot}35$ in, $R = 4{\cdot}953$ in, $E = 10{\cdot}5 \times 10^6$ psi and $\nu = 0{\cdot}3125$. This pinched cylinder problem has been studied in a number of finite element investigations. Most of these are concerned with a shell thickness of 0·094 in. ($R/h = 52{\cdot}8$)[26–30] but there also exist solutions corresponding to a thickness of 0·01548 in. ($R/h = 320$)[29, 30]. The problem is almost inextensional and is sensitive to the representation of rigid-body motions: an inextensional solution by Timoshenko exists[31] though this gives a somewhat low value for the deflection under load. The problem is complicated by the very steep bending moment gradients local to the loading points and it is desirable to take account of this by employing some refinement of the finite element mesh in this region; such refinement is easy to apply where the elements are of triangular shape.

Since accurate comparative values are available only for the magnitude of the deflection under the load, convergence of this quantity alone is examined for both thicknesses of shell in Table 5. The differences in the quoted comparative values of displacement reflect to some extent at least the small differences in the shell theories used. It is seen that convergence of the finite element results is rapid and that very few elements in the symmetric octant are required for a

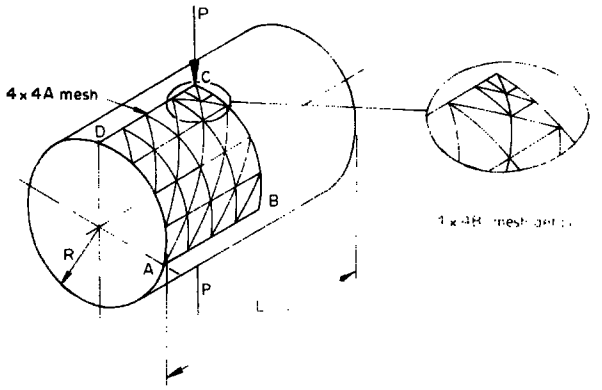

Fig. 9. The pinched cylinder.

Table 5. Deflection of free pinched cylinder

Finite element mesh	Final degrees of freedom	Deflection under load (in.)	
		R/h = 52.8 P = 100 lb.	R/h = 320 P = 0.1 lb.
1 x 1	30	0.10619	0.023217
2 x 2	96	0.11202	0.024236
3 x 3	198	0.11313	0.024453
4 x 4	336	0.11341	0.024536
5 x 5	510	0.11363	0.024621
4 x 4A	374	0.11360	0.024605
4 x 4B	412	0.11364	0.024618
Comparative solutions		0.1135 [30] 0.1137 [29] 0.1139 [28]	0.02462 [30] 0.02439 [25]

result of adequate engineering accuracy. It is noted that results for nearly-inextensional arch problems and particularly for the pinched ring problem [2] indicate that shell elements based on independently-interpolated polynomial displacements in which the membrane components are restricted to a cubic variation will not deal very efficiently with the free pinched cylinder problem.

Pinched cylinder with supported ends

For this problem reference may again be made to Fig. 9 where in this case $L/R = 2$, $R/h = 100$, $\nu = 0{\cdot}3$. Here, though, the cylinder ends are supported by a diaphragm (i.e. the displacement components W and V are zero around the curved edge AD) which increases the problem difficulty. Detailed solutions of this problem based both on a finite element study using their 36 dof element and on a double Fourier series solution are given by Lindberg *et al.* [11].

The finite element results for the 54 dof cylindrical shell element are given in the form of typical distributions of displacement components (Fig. 10) and of forces and moments (Fig. 11) and compared with the solutions of [11]. In considering uniform meshes there is clearly a very significant improvement on an element basis in using the present element and there is also an improvement in the calculated deflection under load (and hence the strain energy) on a degree-of-freedom basis. The very considerable oscillation in the membrane force distribution calculated using the 36 dof element is drastically reduced in using the higher-order element. With regard to the force distributions it is noted that the calculated finite element values of membrane force local to the applied load are converging on rather higher levels than those given by the Fourier series solution. Of course, here again, to make effective use of the refined 54 dof element some grading of the mesh should be used in the region of steep force and moment gradients. It can be seen from Figs. 10 and 11 that when this is done considerable improvement in accuracy results, to the extent that the calculated strain energy for the 4×4A mesh solution differs only by 0·31% compared with the Fourier series solution. (Note that the 2×2A mesh is basically a uniform 2×2 mesh but has the same kind of refinement in the rectangle local to the applied load as is shown for the 4×4A mesh in Fig. 9).

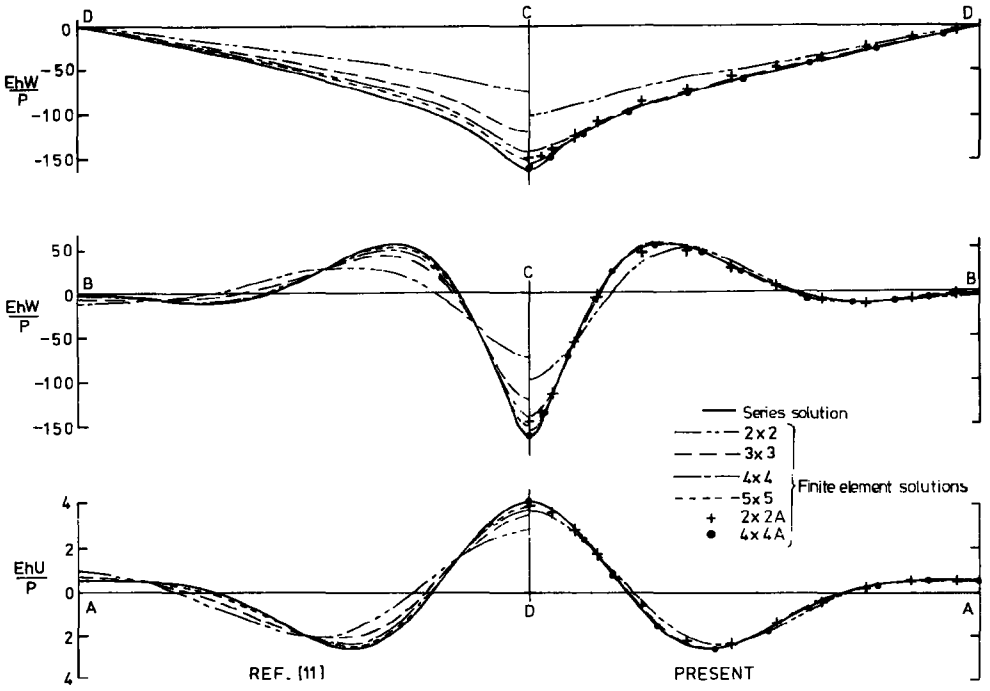

Fig. 10. Supported pinched cylinder. displacement distributions.

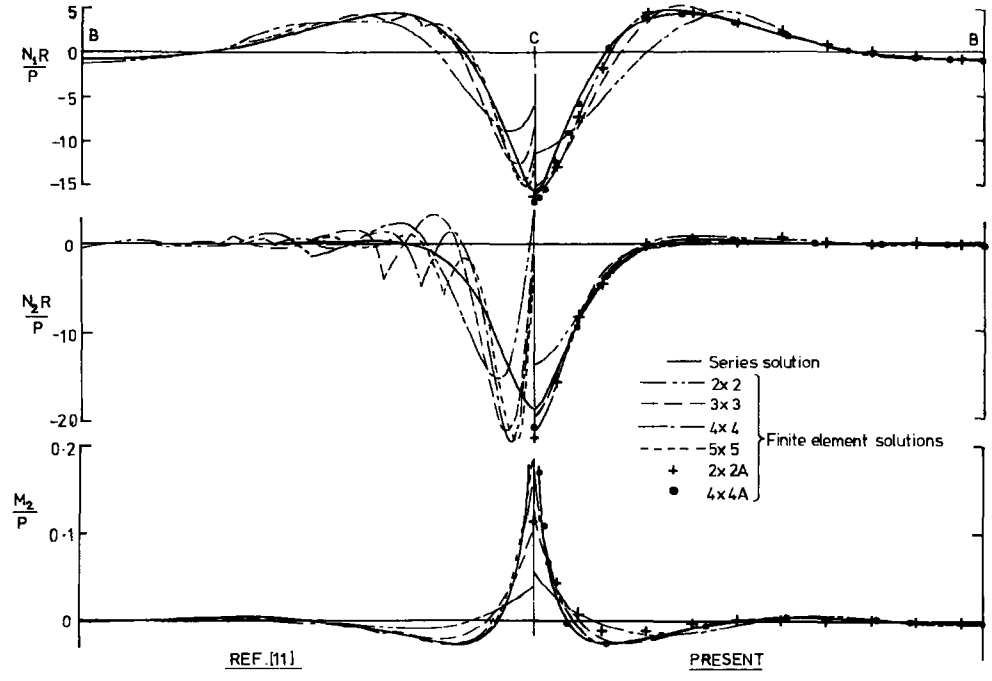

Fig. 11. Supported pinched cylinder. distributions along BC.

4. CONCLUSIONS

The numerical results indicate the high accuracy which can be obtained in a wide range of shell problems using a conforming, triangular finite element formulated in terms of conventional shell theory and based on polynomial surface displacement components which are each of constrained-quintic order. From the results presented here and from those of the limiting case of the arch it is concluded that the 54 dof element is generally more efficient than are elements which have some or all polynomial displacement components of lower order. In particular whilst the

efficiency of the 54 dof element will perhaps differ little in some shallow-shell applications from that of a related 36 dof element (with cubic membrane components), there can be very significant gains in efficiency in applications involving shells of deep, thin geometry. The oscillation or waviness of calculated displacement, force or moment distributions which appears characteristic of comparatively high-order, curved, displacement elements is significantly reduced in the 54 dof element.

As with other high-order displacement elements the use of the present element involves connection of displacement derivatives at the nodes whose compatibility is not required by the variational formulation. From the results obtained here and those obtained earlier for arches this over-compatibility does not appear to lead to any significant excess stiffness. In some circumstances the connection of particular displacement derivatives will need to be relaxed to accommodate some specific physical condition of the shell.

Acknowledgements—The numerical results presented in this paper were obtained using the computing facilities of the Central Electricity Generating Board at Berkeley Nuclear Laboratories, Berkeley, Gloucestershire. The support of this work by the Board is gratefully acknowledged and particular thanks are due to Mr. T. K. Hellen for his help in incorporating the shell elements into the BERSAFE finite element system.

REFERENCES

1. D. J. Dawe, Curved finite elements for the analysis of shallow and deep arches. *Computers and Structures* **4**, 559 (1974).
2. D. J. Dawe, Numerical studies using circular arch finite elements. *Computers and Structures* **4**, 729 (1974).
3. J. H. Argyris and D. W. Scharpf, The SHEBA family of shell elements for the matrix displacement method. *Aero J.* **72**, 873 (1968).
4. G. Dupuis and J. J. Goël, A curved finite element for thin elastic shells. *Int. J. Solids Struct.* **6**, 1413 (1970).
5. A. J. Morris, A deficiency in current finite elements for thin shell applications. *Int. J. Solids Struct.* **9**, 331 (1973).
6. G. Dupuis, Application of Ritz's method to thin elastic shell analysis. *J. Appl. Mech.* **38**, 987 (1971).
7. D. J. Dawe, Rigid-body motions and strain-displacement equations of curved shell finite elements. *Int. J. Mech. Sci.* **14**, 569 (1972).
8. L. S. D. Morley, Polynomial stress states in first approximation theory of circular cylindrical shells. *Q. J. Mech. App Math.* **XXV**, Part 1, 13 (1972).
9. G. R. Cowper, G. M. Lindberg and M. D. Olson, A shallow shell finite element of triangular shape. *Int. J. Solids Struct.* **6**, 1133 (1970).
10. G. M. Lindberg and M. D. Olson, A high-precision triangular cylindrical shell finite element. *AIAA J.* **9**, 530 (1971).
11. G. M. Lindberg, M. D. Olson and G. R. Cowper, New developments in the finite element analysis of shells. National Research Council of Canada DME/NAE Quarterly Buttetin No. 1969(4).
12. G. R. Cowper, G. M. Lindberg and M. D. Olson, Comparison of two high-precision triangular finite elements for arbitrary deep shells. *Proc. 3rd Conf. on Matrix Methods in Struct. Mech.* Wright-Patterson Air Force Base, Ohio (1971).
13. I. Fried, Basic computational problems in the finite element analysis of shells. *Int. J. Solids Structures* **7**, 1705 (1971).
14. I. Fried, Shape functions and the accuracy of arch finite elements. *AIAA J.* **11**, 287 (1973).
15. T. Moan, A note on the convergence of finite element approximations for problems formulated in curvilinear coordinate systems. *Computer Meth. Appl. Mech. Eng.* **3**, 209 (1974).
16. S. Idelsohn, Analyse statique et dynamique des coques par la méthode des élements finis. Ph.D. thesis, University of Liège, Belgium (1974).
17. W. T. Koiter, A consistent first approximation in the general theory of thin elastic shells. In *Theory of Thin Elastic Shells* (Edited by W. T. Koiter). North-Holland, Amsterdam (1960).
18. O. C. Zienkiewicz, *The Finite Element Method*. McGraw-Hill, New York (1971).
19. T. K. Hellen, BERSAFE (Phase 1) A computer system for stress analysis. Part 1: Users' guide. C.E.G.B. Report RD/B/N1761 (1970).
20. S. A. Ambartsumyan, On the calculation of shallow shells. NACA TM 1425 (1956).
21. A. C. Scordelis and K. S. Lo, Computer analysis of cylindrical shells. *J. Am. Concrete Inst.* **61**, 539 (1964).
22. K. Forsberg, An evaluation of finite difference and finite element techniques for analysis of general shells. *Symp. on High Speed Computing of Elastic Struct.* IUTAM, Liège (1970).
23. O. C. Zienkiewicz, R. L. Taylor and J. M. Too, Reduced integration technique in general analysis of plates and shells. *Int. J. Num. Meth. Engng.* **3**, 275 (1971).
24. R. W. Clough and R. J. Johnson, A finite element approximation for the analysis of thin shells. *Int. J. Solids Struct.* **4**, 43 (1968).
25. G. E. Strickland and W. A. Loden, A doubly-curved triangular shell element. *Proc. 2nd Conf. Matrix Methods in Struct. Mech.* Wright-Patterson Air Force Base, Ohio (1968).
26. F. K. Bogner, R. L. Fox and L. A. Schmit, A cylindrical shell discrete element. *AIAA J.* **5**, 745 (1967).
27. G. Cantin and R. W. Clough, A curved, cylindrical shell, finite element. *AIAA J.* **6**, 1057 (1968).
28. G. Cantin, Rigid body motions in curved finite elements. *AIAA J.* **8**, 1252 (1970).
29. D. G. Ashwell and A. B. Sabir, A new cylindrical shell finite element based on simple independent strain functions. *Int. J. Mech. Sci.* **14**, 171 (1972).
30. R. D. Henshell, T. J. Bond and J. O. Makoju, Ring finite elements for axisymmetric thin shell analysis. *Proc. Conf. Variational Methods in Engineering*. University of Southampton (1972).
31. S. P. Timoshenko and S. Woinowsky-Krieger, *Theory of Plates and Shells* 2nd Edn. McGraw-Hill, New York (1959).